3,4:9,10-Perylenetetracarboxylic dianhydride (PTCDA) by electron crystallography

Tetsuya Ogawa,[a]* Kiyoshi Kuwamoto,[a] Seiji Isoda,[a] Takashi Kobayashi[a] and Norbert Karl[b]

[a]*Institute for Chemical Research, Kyoto University, Uji, Kyoto-fu 611-0011, Japan, and* [b]*3. Physikalisches Institut, Universität Stuttgart, Pfaffenwaldring 57, D70550 Stuttgart, Germany. E-mail: ogawa@eels.kuicr.kyoto-u.ac.jp*

Abstract

The crystal structures of the α and β modifications of PTCDA were analyzed as projected structures along the a axes by electron crystallography using an imaging plate. The results for the α modification agree well with the sheet-and-stack structure obtained by X-ray diffraction by M. L. Kaplan *et al.* (private communication, full set of crystal structure data). Projected onto the (102) plane, which is parallel to the molecular sheets, the long molecular axis makes an angle of 42° with the b axis and the hexagonal benzene rings appear slightly elongated, indicating a slight inclination of the molecular plane from the (102) lattice plane. For the β modification, it was concluded that the molecules are aligned in a herringbone packing scheme on the (102) plane similar to that of the α modification, but with a slightly different angle of the long molecular axis with the b axis (38°).

1. Introduction

There has been increasing interest in thin films of organic materials because of their potentially useful electrical and optical properties. To understand the characteristic electrical and optical behavior in detail knowledge of the crystal structure is indispensable. Organic thin films, however, frequently grow with crystal structures different from that of the bulk material. The crystal structures of such thin-film samples can hardly be determined by the X-ray or neutron diffraction experiments usually used for crystal structure analysis. Electron diffraction techniques may be useful for analyzing the crystal structure of such thin films, but mostly only geometrical analysis, such as the determination of the lattice parameters and the space group, has been carried out so far. Structure analysis using diffraction intensities has only rarely been performed because of the difficulties of a theoretical treatment of dynamical scattering and the usually poor precision of the intensity data. However, in recent years, for example, Dorset *et al.* showed that a quantitative structure analysis using electron diffraction intensities can be carried out to some extent with a purely kinematical treatment of the intensities (Dorset, 1995). These workers demonstrated that a rough crystal structure could be obtained by electron crystallography.

In our laboratory, we have also been trying to apply electron crystallography to the analysis of the crystal structures of thin-film organic specimens using an imaging plate (IP) detector (Ogawa *et al.*, 1994*a,b*). The IP is a newly developed recording medium with high sensitivity, wide dynamic range and good linear response between the diffraction intensity and the read-out signal (Isoda *et al.*, 1991). The wide dynamic range is especially suitable for detecting electron diffraction intensities because these appear over a wide intensity range. Moreover, the high sensitivity of the IP makes it possible to reduce the electron dosage applied to the specimen. This is of prime importance in our experiments, since organic materials are generally damaged under electron irradiation. The good linear response is also valuable for measuring intensity data more precisely than with conventional electron-microscope films. To elucidate the applicability of this technique we have recently shown the results of electron crystal structure analysis, using an IP, of graphite and polyethylene single crystals with simple structures (Ogawa *et al.*, 1994*a*), and C$_{60}$ (Ogawa *et al.*, 1997). In this paper, we describe the results of the crystal structure analysis of 3,4:9,10-perylenetetracarboxylic dianhydride (PTCDA, Fig. 1), which exhibits polymorphism and has a more complicated molecular structure than graphite or polyethylene, using electron diffraction intensities.

PTCDA is a commercial red pigment. Its electrical properties have been studied extensively by Forrest *et al.* (Forrest *et al.*, 1984, 1985, 1986; So *et al.*, 1990). A full single-crystal structure analysis of one of the polymorphs was carried out by Kaplan *et al.* (M. L. Kaplan *et al.*, private communication; Lovinger *et al.*, 1984). Möbus *et al.* (1992) studied the epitaxic growth of PTCDA deposited on alkali-halide substrates by elec-
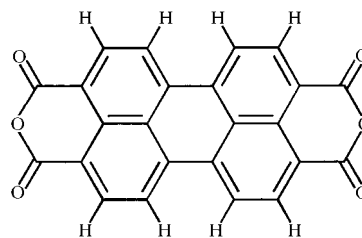

Fig. 1. 3,4:9,10-Perylenetetracarboxylic dianhydride (PTCDA).

tron microscopy. They found two polymorphs in the commercially supplied powder and thin epitaxic films obtained by vacuum deposition. One polymorph, subsequently named the α modification, had the same structure as the sample analyzed by Kaplan *et al.* The other new polymorph was consequently named the β modification. The α modification crystallizes in the space group $P2_1/c$ with lattice constants $a = 0.374$, $b = 1.196$, $c = 1.734$ nm and $\beta = 98.8°$. The β modification was found to crystallize in the same space group, $P2_1/c$, but with different lattice parameters: $a = 0.378$, $b = 1.930$, $c = 1.077$ nm and $\beta = 83.6°$. The packing of the planar molecules in the unit cell of the β modification was deduced from that of the α modification by assuming a different stacking scheme of the molecular sheets so as to explain the observed X-ray powder intensities. Fig. 2 shows schematic diagrams of the α and β structures following Möbus *et al.* (1992). In both modifications, the planar molecules lie almost flat on the (102) lattice planes with only slight inclinations, which are probably caused by a steric effect. The two symmetry-related molecules in each unit cell are arranged in a herringbone packing in each (102) lattice plane and both crystals are composed of stacks of such sheets, with a slight shift towards the shorter side of the (102) cross section of the unit cell for the α modification and towards the longer side for the β modification in subsequent sheets.
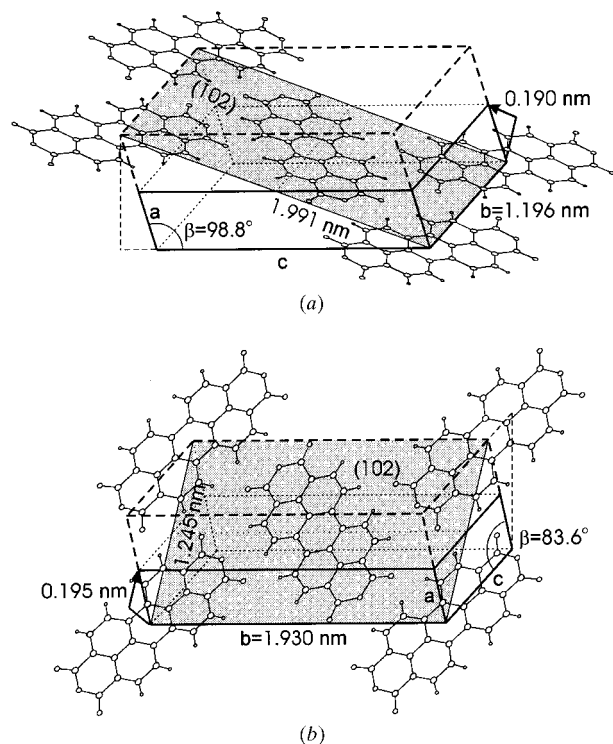

Fig. 2. The expected packing of PTCDA in the lattice for (*a*) the α modification and (*b*) the β modification.

We observed electron diffraction patterns obtained with the electron beam along the *a* axis (*i.e.* for the b^*c^* reciprocal lattice plane) for both the α and β modifications and analyzed the structures projected on the plane normal to the *a* axis using the structure amplitudes and phases determined by a direct phasing procedure with a kinematical treatment.

2. Methods and materials

A microscopy sample was prepared by vacuum deposition under a vacuum of 1×10^{-5} Pa onto a KCl substrate held at 453 K after baking the substrate at 673 K for 1 h. The thickness of the sample was estimated to be about 10 nm using a quartz crystal oscillator. After reinforcement of the sample by an overlayer of amorphous carbon, the film was stripped off by water and the floating film was taken over onto an electron microscope grid.

The transmission electron microscope (TEM) used was the Jeol JEM-ARM1000 at the Institute for Chemical Research of Kyoto University, Japan. It was operated at an acceleration voltage of 1000 kV. Such high voltage is useful for reducing radiation damage of the specimen by electron beam dosage and also for diminishing dynamical effects in electron diffraction relative to that caused in a normal 100–200 kV TEM. Moreover, the Ewald sphere is very large because of the very short wavelength of the electrons, so that each reciprocal lattice can be assumed to be cut by a plane. The specimen was tilted by about 30° for the α or β modifications to observe each b^*c^* diffraction pattern.

DL-UR$_{III}$ (Fuji Film) imaging plates with an active area of 102×77 mm^2 were used for recording the electron diffraction. Recording and reading of the diffraction intensities were carried out using PIXsysTEM, an imaging-plate system supplied by Jeol. The read-out image consists of 2048×1536 pixels. Each pixel is 50×50 μm^2 and the read-out values range from 0 to 4095 (these values are proportional to the logarithm of the electron dose).

Fig. 3 indicates the procedure of the present structure analysis. The transformation of the read-out signal to an electron intensity was based on previously determined data obtained in checking the linearity between the read-out signal and the logarithm of the dosage (Isoda *et al.*, 1991). The intensities obtained were digitized and integrated after correction for the background, which was estimated by a least-squares fit of the background scattering in a doughnut-shaped region around each spot. Because the *a*-axis projected structure shows a two-dimensional *pgg* symmetry for both modifications, four or two symmetry-equivalent reflections can be obtained; the equivalent intensities of such reflections were averaged.

A preliminary scaling factor and a temperature factor were determined by a Wilson plot, and redetermined

later as parameters in the least-squares refinement procedure. Using these factors, normalized structure factors were calculated and the phases for the structure factors were determined by a direct phasing procedure. The Σ_2 relationship was used in the procedure. A two-dimensional potential map for the crystal structure projected along the a axis was synthesized from the structure amplitudes and the phases. Atomic positions were determined from the peak positions in the map. A least-squares fit was then carried out to refine the structural parameters using the scaling factor, the temperature factors and the peak positions (corresponding to atoms) in the potential map as the initial values.

3. Results and discussion

Fig. 4 shows an electron micrograph of PTCDA crystals deposited on a KCl substrate (001) surface at 453 K. Needle-like planar crystallites of the α and β modifications were epitaxially grown with their (102) planes parallel to the substrate (Möbus *et al.*, 1992). Narrower needle-like crystals (indicated by α in Fig. 4) turned out to be the α modification and wider or plate-like crystals (β in Fig. 4) turned out to be the β modification. The long axis of the crystal of the α modification is along its b axis, and that of the crystal of the β modification is along the [$\bar{2}$01] direction, making an angle of 24° with the [100] direction of the (001) KCl surface; these are the shorter axes of the unit mesh of each (102) sheet. Since the mesh plane (102) is parallel to the surface of the substrate, $b*c*$ diffraction could be obtained by tilting the sample by about 30° around these axes.

3.1. *The structure of the α modification*

Fig. 5 shows a $b*c*$ electron diffraction pattern of the α modification recorded on an IP with an incident electron dose of 4×10^{-5} C cm^{-2}. The intensities could be measured over a range of about four decades with the IP. Although some odd-order forbidden reflections appear on the $b*$ and $c*$ axes, these are weak in intensity and may arise from a dynamical effect or structural disorder in the crystal, so we ignored them in the present kinematical treatment. From this image, 177 integrated intensities of symmetry-independent reflections were obtained from the 621 measured intensities after averaging the symmetry-equivalent reflections. The outermost spot represents a Bragg spacing of 0.074 nm.
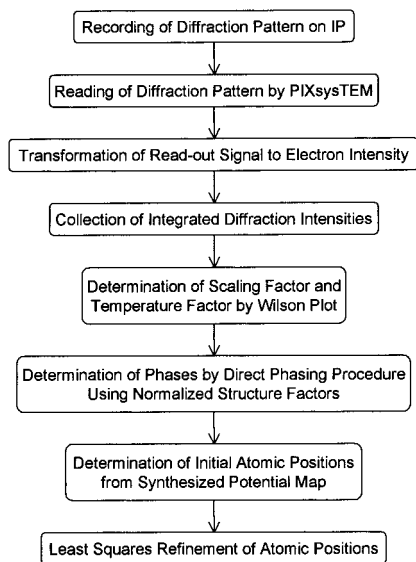

Fig. 3. A scheme showing the present structure analysis by electron diffraction.

Fig. 4. An electron micrograph of PTCDA crystallites deposited on a KCl substrate at 453 K.
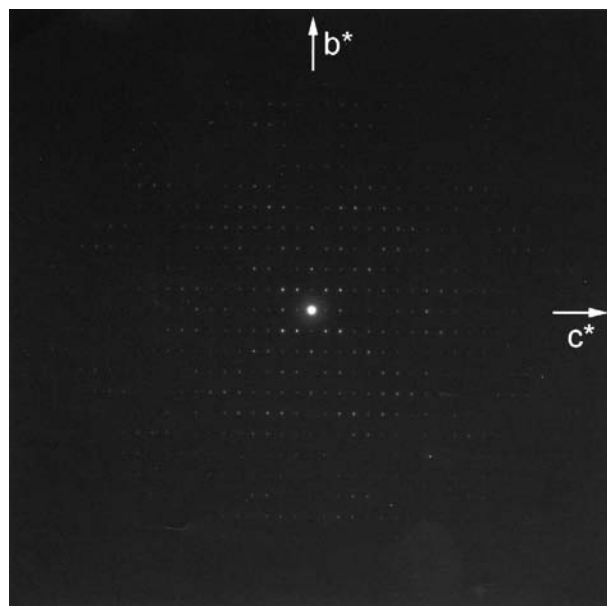

Fig. 5. The electron diffraction pattern of the α modification of PTCDA with the electron beam incident along the crystalllographic a axis.

Table 1. *Comparison of observed and calculated structure factors for the α modification of PTCDA*

48 principal reflections are tabulated together with the strong reflections used for the direct phasing procedure. $|E|$ are the normalized structure factors and the phases are given as determined by the direct phasing procedure. F_{calc} are obtained by the final least-squares fit.

h	k	l	$|E|$	Phase	$|F_{obs}|$	F_{calc}	h	k	l	$|E|$	Phase	$|F_{obs}|$	F_{calc}
0	1	1	1.05	0	58.20	56.90	0	10	3	1.98	0	19.26	19.27
0	0	2	0.48	—	37.27	40.19	0	3	14	1.28	0	12.43	12.35
0	1	2	1.30	π	69.06	−69.06	0	6	12	1.76	0	16.85	16.54
0	2	0	0.60	—	44.14	−44.87	0	4	14	1.88	0	16.94	22.37
0	2	3	0.58	—	26.57	23.90	0	10	5	1.48	0	13.20	5.64
0	3	2	0.78	—	33.47	−27.58	0	10	6	1.44	π	12.15	−5.95
0	2	4	0.94	—	39.22	−39.45	0	3	15	1.78	0	14.91	18.45
0	4	0	0.57	—	30.59	30.59	0	7	12	1.18	π	9.82	−10.70
0	5	2	1.23	0	36.60	33.90	0	4	15	1.37	0	10.64	10.82
0	0	8	0.90	—	35.11	−35.11	0	9	10	1.04	π	7.81	−4.12
0	5	3	1.54	π	43.70	−43.01	0	7	13	1.30	0	9.56	11.27
0	4	6	1.16	π	30.50	−55.19	0	11	5	1.05	π	7.59	−7.51
0	5	5	1.25	π	30.76	−31.17	0	3	16	1.64	0	11.80	6.78
0	4	7	1.12	π	26.29	−19.20	0	8	12	1.63	π	11.63	−7.83
0	6	3	1.01	0	23.38	23.43	0	11	6	1.82	0	12.47	3.28
0	1	9	1.18	π	27.34	−32.05	0	1	17	1.23	π	8.17	−6.37
0	6	4	1.15	π	25.29	−24.46	0	2	17	1.35	0	8.77	5.72
0	5	10	1.09	π	15.41	−7.86	0	11	7	1.03	π	6.70	−8.93
0	6	10	1.21	0	14.80	12.63	0	8	13	1.08	π	6.98	1.00
0	9	3	1.84	0	22.39	21.02	0	9	12	1.87	π	11.56	−9.31
0	9	4	1.86	0	21.72	22.40	0	2	18	1.97	π	10.99	−11.13
0	6	11	2.06	π	22.29	−25.92	0	11	14	1.01	0	3.59	4.26
0	4	13	1.56	0	16.31	20.49	0	3	22	1.07	π	3.08	−2.16
0	10	2	1.86	0	18.61	24.69	0	7	21	1.97	π	5.01	−2.68

41 reflections with large normalized structure factors were used for the determination of the phases by a direct phasing procedure using the Σ_2 relationship. (The centrosymmetry of this *a*-axis projection of the unit cell means that the structure factors are real numbers. Therefore, the determination of the phases is simply the determination of the signs of the structure factors.) The signs of the structure factors determined by this procedure are shown in Table 1. Fig. 6 is the potential map synthesized from these 41 diffraction amplitudes and phases. Although there are a number of artificial weak peaks, stronger peaks are attributed to the C and O atoms of the known molecular structure. The peak positions were used as the initial parameters for the following structure refinement by least-squares fit using all 177 diffraction data. Least-squares refinement of the scaling factor, the isotropic temperature factor and the atomic positions was carried out. As the H-atom positions did not converge to physically reasonable values, we assumed rigid positions for these atoms by setting the
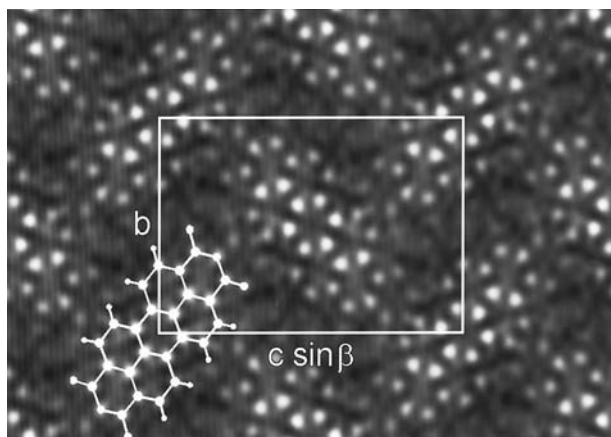

Fig. 6. The potential map projected along the *a* axis for the α modification. This map was synthesized from 41 structure factors, the signs of which were determined by a direct phasing procedure.
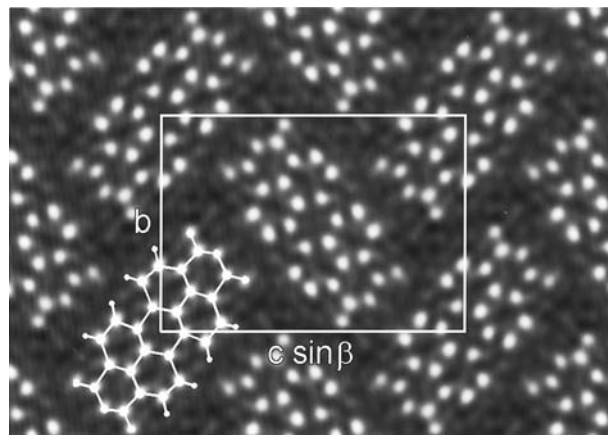

Fig. 7. The refined potential map projected along the *a* axis for the α modification. This map was synthesized from the full set of 177 observed structure factors with the signs of the theoretical structure factors calculated from the atomic positions obtained by a least-squares fit.
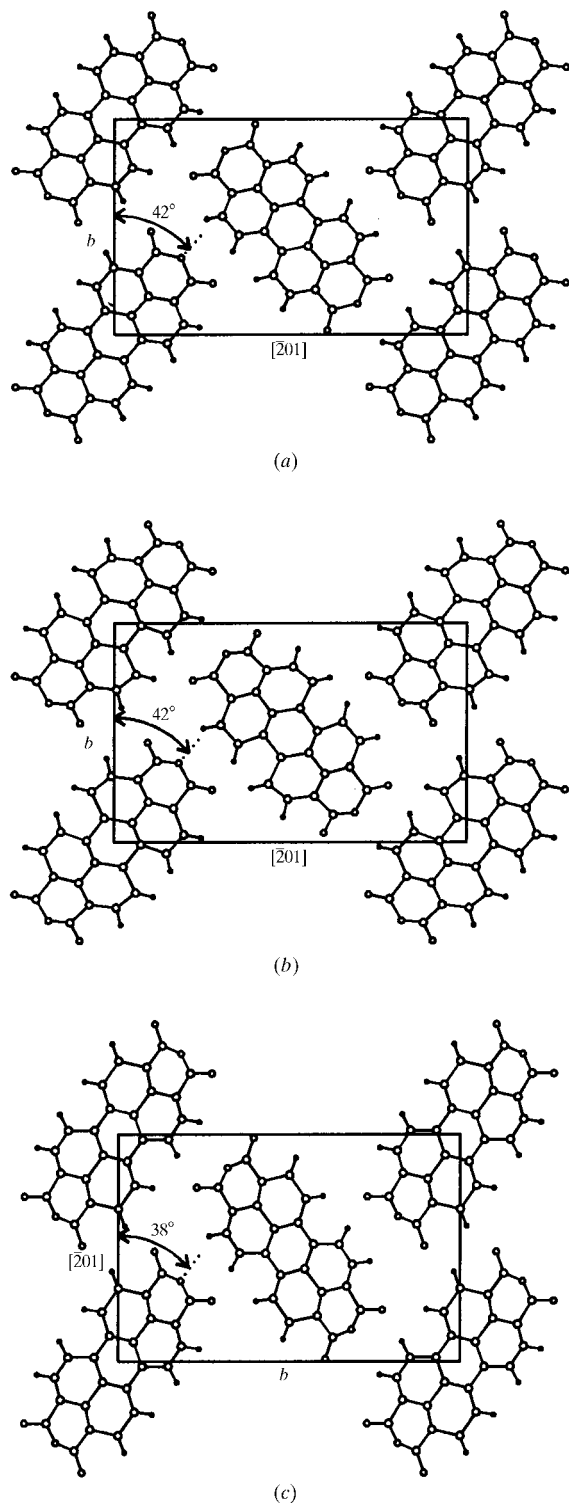
(a)

(b)

(c)

Fig. 8. A projection of the atomic positions onto the (102) plane (a) from the X-ray data of M. L. Kaplan *et al.*, and our results from electron diffraction for (b) the α modification and (c) the β modification.

Table 2. *Two-dimensional atomic coordinates of PTCDA determined by the least-squares refinement*

	α modification		β modification	
	y	z	y	z
C	−0.020	0.076	−0.021	0.112
C	0.110	−0.025	0.073	−0.013
C	0.089	0.048	0.048	0.097
C	−0.045	0.147	−0.050	0.222
C	0.227	−0.053	0.142	−0.029
C	0.181	0.095	0.096	0.190
C	0.044	0.195	0.004	0.314
C	0.316	−0.003	0.184	0.066
C	0.151	0.167	0.070	0.298
C	0.292	0.068	0.167	0.171
C	0.247	0.218	0.125	0.387
C	0.379	0.120	0.214	0.266
O	0.355	0.190	0.190	0.382
O	0.219	0.280	0.099	0.512
O	0.481	0.100	0.276	0.261

C—H bond length to 0.1 nm and the C—C—H angle to the same for both sides of the C—H bond on the (102) plane. Some of the final fitted structure-factor values are tabulated in Table 1. The two-dimensional atomic coordinates are shown in Table 2. The final temperature factors were 0.026 nm² for the C atoms and 0.047 nm² for the O atoms, and an R factor of 0.204 was reached. Fig. 7 shows the potential map synthesized from the observed structure factors with the signs calculated from the result of the least-squares fit. C and O atoms are more distinguishable as isolated peaks than in Fig. 6.

Assuming that the molecule is planar, the structure on the (102) plane can be derived from the projected potential map along the *a* axis. Fig. 8 shows three projections of the atomic positions onto the (102) plane derived from (a) the results of the X-ray crystal structure determination by M. L. Kaplan *et al.*, (b) our electron diffraction results for the α modification and (c) our electron diffraction results for the β modification, described in §3.2. All the projections show a slightly deformed hexagon for the benzene rings because in all cases the molecule is slightly inclined relative to the (102) plane. Table 3 compares the bond lengths and angles for these three projections.

Although the R factor is not as small as that obtained in the X-ray experiment and the atomic positions exhibit a small displacement from those of the X-ray results, the angle between the longer axis of the molecule and the *b* axis in the case of the α modification, which is 42°, agrees well with the results of the X-ray experiment (see Fig. 8). The rather large R factor is common for structure analysis by electron crystallography and an R value less than 0.20 may be said to be very good. The reason for this is thought to arise partly from the dynamical scattering effect and mainly from the slight bending of the thin crystal in the present case. In fact, the diffraction pattern shows weak forbidden reflections which may result from these effects. In our sample, the crystallites

Table 3. *Ranges of bond lengths (nm) and angles (°) obtained for the PTCDA molecule from the structure projected onto the (102) plane*

	α modification		β modification
	M. L. Kaplan *et al.*	This work	This work
C−C	0.138–0.152	0.128–0.161	0.125–0.161
C−O	0.140, 0.146	0.138, 0.123	0.114, 0.120
C=O	0.123, 0.119	0.121, 0.114	0.126, 0.122
C−C−C	116.0–123.6	101.4–135.9	108.9–132.3
C−O−C	126.6	125.1	138.4
C−C−O	116.2, 117.9	112.5, 131.3	104.2, 122.4
O−C=O	118.5, 117.1	131.7, 123.1	132.1, 116.4

are so thin that some distortion from bending must be assumed, which gives a slight deviation from the Bragg condition in some regions of the crystal. Dynamical scattering simulation by the multi-slice method shows that the *R* factor is not improved by including such an effect in the calculation. No intensity arises for the forbidden reflections on the *b** and *c** axes at the present crystal thickness when the *a* axis is parallel to the electron beam. For slight deviations from the beam direction, however, it is shown that the forbidden reflections have some intensity on the *b** and *c** axes even for crystals only a few hundred ångströms thick. Therefore, the dynamical scattering effects are small in the present case and the forbidden reflections are considered to arise mainly from the structural disorder in the ultra-thin crystals, which violates the symmetric condition for the extinction rule.
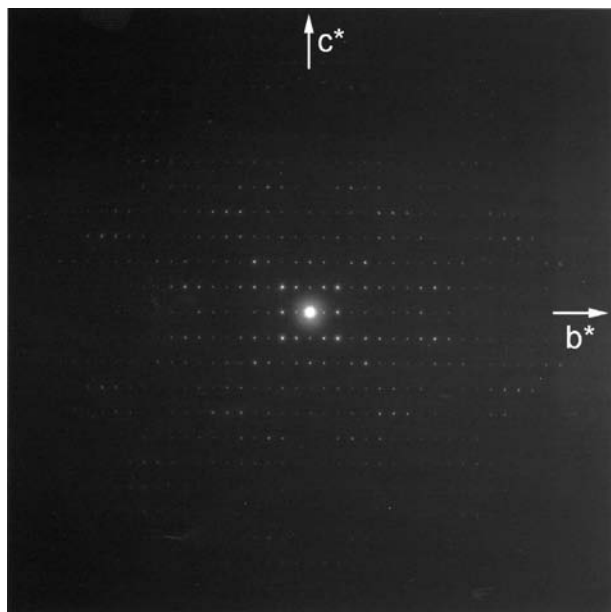
3.2. *The structure of the β modification*

The structure of the β modification was analyzed as for the α modification. Fig. 9 shows the *b**c** diffraction pattern of the β modification. The intensities of 183 symmetry-independent reflections were obtained by symmetry averaging of the 675 measured intensities. The outermost reflection corresponds to a Bragg spacing of 0.090 nm.

The 43 normalized structure factors with large values used for the determination of the phases by applying a direct phasing procedure, and those of nine additional principal reflections, are given in Table 4. (An asterisk next to a phase indicates that the phase determined by the direct phasing procedure is inconsistent with the final least-squares results.) Fig. 10 shows the potential map synthesized from these 43 structure factors. The atomic positions read from this map were used as initial values for a least-squares refinement. The refinement leads to an *R* factor of 0.265 with temperature factors of 0.055 nm^2 for the C atoms and 0.068 nm^2 for the O atoms. Fig. 11 shows the potential map synthesized from the observed structure factors with the calculated structure-factor signs.

Bond lengths and angles for the structure projected onto the (102) plane are shown in Table 3. Fig. 8(*c*) shows the projection of the atomic positions onto the (102) plane — the molecular packing of the β modification in the (102) plane. It is indeed similar to that of the α modification as deduced by Möbus *et al.* (1992): in fact, the molecules lie almost parallel to the (102) plane. The longer axis of the molecule makes an angle of 38° with the [2̄10] shorter axis of the (102) mesh plane. The elongation of the hexagons of the benzene rings along the [2̄10] direction may arise from a slight inclination of the molecular plane relative to the (102) lattice plane in a similar way to that in the α modification, but the somewhat larger elongation indicates a slightly larger inclination in the β modification than in the α modification. This agrees well with the X-ray results: Möbus *et al.* (1992) expected the inclinations to be ~5 and ~10° for the α and β modifications, respectively.

Fig. 9. The electron diffraction pattern of the β modification with the electron beam incident along the crystallographic *a* axis.
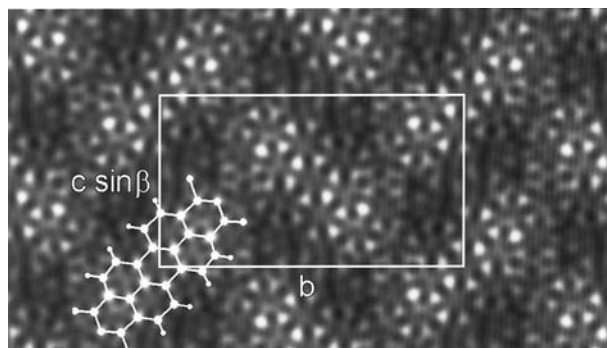

Fig. 10. The potential map projected along the *a* axis for the β modification. This map was synthesized from 43 structure factors, the signs of which were determined by a direct phasing procedure.

Table 4. *Comparison of observed and calculated structure factors for the β modification of PTCDA*

52 principal reflections are tabulated together with those used for the direct phasing procedure. $|E|$ are the normalized structure factors and the phases are given as determined by the direct phasing procedure. F_{calc} are obtained by the final least-squares fit. Phases marked with an asterisk are inconsistent with the final least-squares results.

h	k	l	$|E|$	Phase	$|F_{obs}|$	F_{calc}	h	k	l	$|E|$	Phase	$|F_{obs}|$	F_{calc}
0	2	0	0.87	—	79.35	46.42	0	4	9	1.01	0	6.50	6.79
0	1	1	0.91	0	58.39	55.45	0	16	3	1.79	0	11.10	12.16
0	2	1	1.60	π	97.99	−84.95	0	13	6	1.27	π	7.84	−7.05
0	0	2	0.39	—	31.80	−31.83	0	17	1	1.13	0*	6.74	−3.05
0	1	2	0.39	—	21.67	18.46	0	17	2	1.93	0	10.84	5.46
0	4	1	0.76	—	39.80	39.79	0	1	10	1.60	0	7.81	11.14
0	3	2	0.48	—	24.51	18.73	0	13	7	1.30	0	6.26	6.60
0	5	1	0.57	—	27.15	27.14	0	11	8	1.33	π	6.38	−1.30
0	4	2	1.01	—	47.33	−47.36	0	2	10	1.25	0	5.99	6.96
0	8	0	0.52	—	23.53	−23.53	0	18	2	2.71	π	12.44	−2.56
0	8	1	0.87	—	27.31	21.86	0	12	8	1.98	π	8.33	−5.30
0	5	4	0.92	π	26.17	−33.69	0	14	7	1.28	π	5.28	−6.75
0	9	1	1.46	π	38.99	−43.36	0	6	10	1.10	π	4.41	−3.70
0	6	4	1.01	π	25.89	−47.66	0	10	9	1.23	π	4.88	−0.90
0	3	5	0.95	π	23.96	−23.93	0	19	2	1.27	0	4.73	1.44
0	10	1	0.93	0	20.95	28.95	0	7	10	1.16	0	4.32	2.83
0	13	3	0.94	0	10.19	10.84	0	11	9	1.23	π	4.41	−2.71
0	13	4	1.23	0	11.46	4.47	0	19	3	1.36	π	4.71	−2.97
0	14	3	1.95	0	17.70	10.17	0	18	5	0.91	0	2.89	1.44
0	11	6	1.36	π	11.33	−6.51	0	12	9	1.05	0*	3.29	−2.17
0	14	4	1.52	0	11.91	9.79	0	19	4	1.14	π*	3.46	0.98
0	15	3	2.82	0	21.26	16.98	0	20	3	1.34	0	3.73	2.52
0	12	6	1.72	0	12.43	13.78	0	6	11	1.09	π*	3.03	3.41
0	2	9	1.03	0	7.11	6.95	0	19	5	1.11	π	2.87	−0.57
0	3	9	1.61	0	10.81	11.18	0	7	11	1.16	π	3.01	−1.14
0	15	4	0.98	0	6.39	4.29	0	8	11	1.11	0	2.67	3.65

4. Conclusions

For the α modification of PTCDA, the crystal structure analyzed by the electron diffraction method agrees well with that obtained by X-ray diffraction. The bond lengths and angles obtained display a somewhat larger scatter. However, the characteristics of the molecular packing [*i.e.* not only the molecular orientation but also the apparent strain which is caused by a slight inclination of the molecular plane with respect to (102)] in the
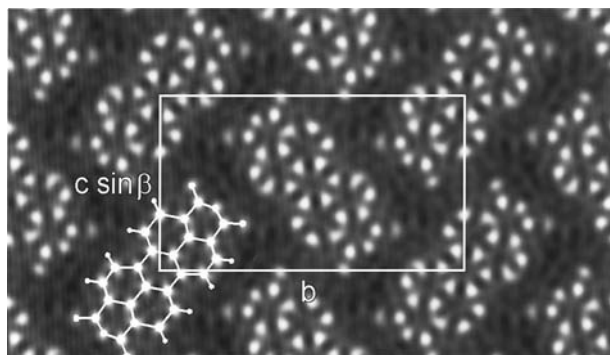

Fig. 11. The refined potential map projected along the *a* axis for the β modification. This map was synthesized from the full set of 183 observed structure factors with the signs of the theoretical structure factors calculated from the atomic positions obtained by a least-squares fit.

molecular projection on the (102) plane could be detected clearly by the electron diffraction method.

We have confirmed the model of Möbus *et al.* (1992) for the β modification, in which the molecules are packed in the (102) lattice plane in the same way as in the α modification.

The packing of organic molecules in a unit cell has been determined in some cases from high-resolution electron microscopy images. However, it is generally difficult to get such images with satisfactory resolution because of electron radiation damage. The electron diffraction method, in contrast, does not need as high an electron dose as is necessary for high-resolution imaging. Moreover, an IP has a higher sensitivity than normal electron-microscope film.

The R factors obtained were not as small as those usually attained in X-ray crystallography because of the stronger interaction of electrons with matter, leading to multiple scattering (dynamical effects). In addition, bending of the tiny crystals needed in electron diffraction may have resulted in deterioration of the quality of the data. In order to obtain more precise results, it is important to avoid dynamical scattering effects by observing crystals which are as thin as possible with an acceleration voltage as high as possible and to reject the influence of crystal bending by using a small selected-area aperture and searching for appropriate bend-free positions of the specimen. However, the results

presented here clearly show that electron crystallography is a useful tool for crystal structure analysis of organic materials that can be prepared as microcrystalline thin films. In addition, it is worth mentioning that organic materials, which are attractive for basic studies of 'molecular electronics', are frequently not available as single crystals large and perfect enough for a full X-ray crystal structure determination.

References

Dorset, D. L. (1995). *Structural Electron Crystallography*. New York, London: Plenum Press.

Forrest, S. R., Kaplan, M. L. & Schmidt, P. H. (1984). *J. Appl. Phys.* **55**, 1492–1507.

Forrest, S. R., Kaplan, M. L. & Schmidt, P. H. (1986). *J. Appl. Phys.* **60**, 2406–2418.

Forrest, S. R., Kaplan, M. L., Schmidt, P. H. & Parsey, J. M. Jr (1985). *J. Appl. Phys.* **58**, 867–870.

Isoda, S., Saitoh, K., Moriguchi, S. & Kobayashi, T. (1991). *Ultramicroscopy*, **35**, 329–338.

Lovinger, A. J., Forrest, S. R., Kaplan, M. L., Schmidt, P. H. & Venkatesan, T. (1984). *J. Appl. Phys.* **55**, 476–482.

Möbus, M., Karl, N. & Kobayashi, T. (1992). *J. Cryst. Growth*, **116**, 495–504.

Ogawa, T., Isoda, S. & Kobayashi, T. (1997). *Acta Cryst.* B**53**, 831–837.

Ogawa, T., Moriguchi, S., Isoda, S. & Kobayashi, T. (1994*a*). *Polymer*, **35**, 1132–1136.

Ogawa, T., Moriguchi, S., Isoda, S. & Kobayashi, T. (1994*b*). *Proceedings of the Thirteenth International Congress on Electron Microscopy*, Vol. 1, pp. 965–966. Les Ulis: Les Editions de Physique.

So, F. F., Forrest, S. R., Shi, Y. Q. & Steier, W. H. (1990). *Appl. Phys. Lett.* **56**, 674–676.